JOURNAL OF PHYSICAL ORGANIC CHEMISTRY, VOL. 9, 573–582 (1996)

AB INITIO MO STUDY OF BENZYLIC CATIONS—2. STERIC EFFECTS ON THE RESONANCE INTERACTION AND ON THE RESONANCE DEMAND IN THE YUKAWA–TSUNO EQUATION

KAZUHIDE NAKATA, MIZUE FUJIO,* YOSHIHIRO SAEKI, MASAAKI MISHIMA AND YUHO TSUNO†
Institute for Fundamental Research of Organic Chemistry, Kyushu University, Fukuoka 812, Japan
AND
KICHISUKE NISHIMOTO*‡
Department of Chemistry, Faculty of Science, Osaka City University, Osaka 558, Japan

Geometries of secondary and tertiary benzylic cations, which have bulky substituents at α positions, were optimized by *ab initio* MO calculations at the RHF/6–31G* and, in part, MP2/6–31G* levels. Calculated ϕ_{calc}, which is the dihedral angle of the α-C – C bond with respect to the aromatic plane, is compared with the relative resonance demand r/r_{max} obtained from solvolysis reactivity and also cation stability; r and r_{max} are the resonance demand in the Yukawa–Tsuno equation for any given system examined and the corresponding ideal full-resonance stabilized demand, respectively. The results suggest that there is a close relationship between the experimental and calculated relative resonance demands expressed by $r/r_{\mathrm{max}} = \cos^2 \phi_{\mathrm{calc}}$, which is suggested by HMO theory for the resonance interaction in the benzyl cation. Thus the r value is a good parameter indicating the degree of resonance interaction between benzylic 2pπ-orbital and the benzene π-system.

INTRODUCTION

In Part 1,[1] we reported some theoretical parameters related to the resonance interaction between the benzylic 2pπ-orbital and the benzene π system and a close linear relationship between these parameters and the resonance demand in the Yukawa–Tsuno (YT) equation. In this work, we studied the effect of steric hindrance on the resonance interaction.

The YT equation:[2]

$$\log(k/k_0) = \rho(\sigma^0 + r\Delta\bar{\sigma}_{\mathrm{R}}^{+}) \tag{1}$$

is one of the most useful tools for characterizing the transition state of reactions affected by the benzene π-system, and has been applied to a wide variety of reaction systems.[3,4] The YT equation is characterized by the resonance demand parameter r, which is a measure of the degree of resonance interaction between the reaction centre and benzene π-system. In previous studies concerning the substituent effect on tertiary benzylic solvolyses, a significant decrease was observed in the r value as the bulkiness of α-alkyl group increases; $r = 0{\cdot}91$ was observed for α-*t*-butyl-α-methylbenzyl,[3i] $r = 0{\cdot}71$ for α-*t*-butyl-α-isopropylbenzyl[3j] and $r = 0{\cdot}26$ for α,α-di-*t*-butylbenzyl[3k] systems, respectively, while $r = 1{\cdot}00$ for the α,α-dimethylbenzyl system by definition. The decrease in the r value may be attributed to the loss of resonance interaction between benzylic 2pπ-orbital and the benzene π system as shown in Figure 1. In the case where the dihedral angle ϕ shown in Figure 2 is 0°, the system acquires full resonance stabilization to provide the maximum r value. Then for the congested system where both 2pπ-orbitals cannot remain parallel owing to steric hindrance, the efficiency of the resonance effect decreases compared with that of the coplanar system, resulting in a decrease in the r value.

---

* Authors to whom correspondence should be addressed.

† Present address: Department of Chemistry, Faculty of General Education, Kumamoto University, Kumamoto 860, Japan

‡ Present address: 1-37-10 Kamotanidai, Sakai City, Osaka 558, Japan

CCC 0894–3230/96/080573–10

Received 19 February 1996
Revised 10 March 1996

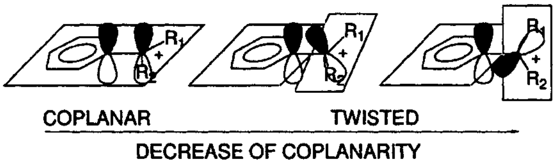

Figure 1. Decrease of resonance interaction due to steric hindrance

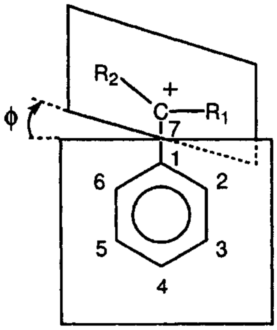

Figure 2. Numbering of atoms for α-substituted benzylic cations

Thus the examination of the dependence of the r value on the dihedral angle ϕ will provide convincing evidence for the origin of the empirical resonance demand parameter r in the YT equation. In substituent effect studies on gas-phase stabilities, the same r values as those in solvolysis were obtained.[4b,4g] This shows that the structure of the transition state in S_N1 solvolysis and the corresponding cation are very similar. Hence one can use a cation as a model of the transition state of S_N1 solvolysis.[1]

The geometries of parent benzylic cations which are both sterically hindered and planar were optimized by *ab initio* MO methods at the RHF/6–31G* and, in part, MP2/6–31G* levels to determine the dihedral angle ϕ of a given cation. The relationships between the r values and calculated dihedral angles ϕ_{calc} were studied to clarify the origin of the r value.

METHOD

The *ab initio* LCAO–MO calculations[5] were carried out for the α-substituted benzyl cations shown in Figure 3.

Details of the optimized structures with respect to cations **2**, **3** and **6–10** were reported previously.[1] All

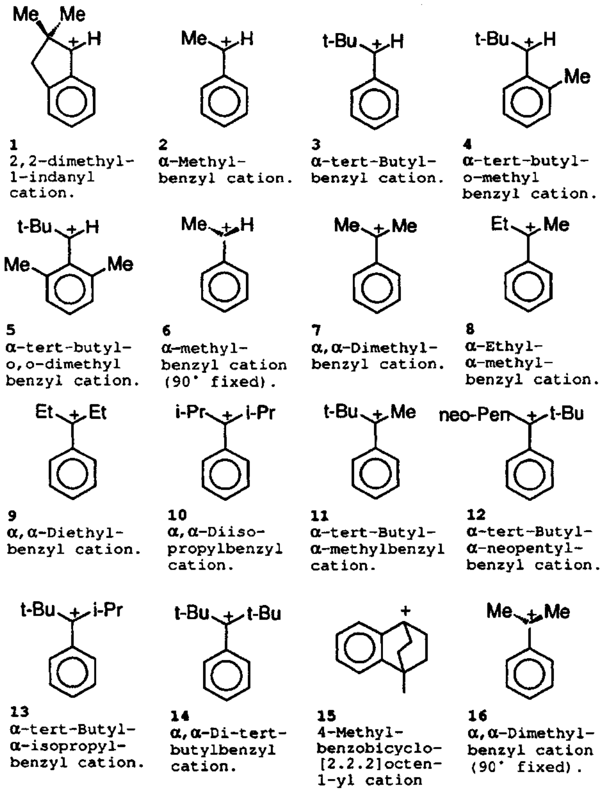

1 2,2-dimethyl-1-indanyl cation.

2 α-Methylbenzyl cation.

3 α-tert-Butylbenzyl cation.

4 α-tert-butyl-o-methyl benzyl cation.

5 α-tert-butyl-o,o-dimethyl benzyl cation.

6 α-methylbenzyl cation (90° fixed).

7 α,α-Dimethylbenzyl cation.

8 α-Ethyl-α-methylbenzyl cation.

9 α,α-Diethylbenzyl cation.

10 α,α-Diisopropylbenzyl cation.

11 α-tert-Butyl-α-methylbenzyl cation.

12 α-tert-Butyl-α-neopentylbenzyl cation.

13 α-tert-Butyl-α-isopropylbenzyl cation.

14 α,α-Di-tert-butylbenzyl cation.

15 4-Methylbenzobicyclo[2.2.2]octen-1-yl cation

16 α,α-Dimethylbenzyl cation (90° fixed).

Figure 3. Calculated benzylic cations (**1**–**16**)

calculations were performed on an IBM RS/6000 computer with the Gaussian-92 suite of programs.[6] The closed-shell restricted Hartree–Fock levels with STO-3G, 3–21G, and 6–31G* basis sets were applied to find stationary points on the potential energy surface (PES) with respect to the twisting angle (dihedral angle ϕ shown in Figure 2) between the benzylic and benzene frameworks. At the RHF/6–31G* level all optimized structures were checked by analysis of harmonic vibrational frequencies obtained from diagonalization of force constant matrices to find the order of the stationary points.

Figure 2 shows the dihedral angle ϕ between $R_1C_7R_2$ plane and benzene framework and also the numbering of atoms. In order to examine the effect of electron correlation on the dihedral angle ϕ, single-point calculation by Møller–Plesset perturbation theory[7] (MP2) for cations **7**, **11**, **12**, **13** and **14** were carried out with the geometries whose dihedral angle ϕ changes by ±5° around the C_1–C_7 axis with the RHF/6–31G* optimized geometry. In the case of **14**, optimization at the MP2/6–31G* level with the frozen core approximation was also achieved in C_2 symmetry. In order to study how the resonance interaction is affected by the change of dihedral angle ϕ, the rotational potentials about the C_1 – C_7 bonds of α,α-dimethylbenzyl and benzyl cations were calculated by geometry optimization techniques, changing the dihedral angles from 0 to 90°. Appropriate functional forms of the resonance interaction energy with respect to dihedral angle ϕ were examined by plotting against the potential energy.

RESULTS AND DISCUSSION

Geometries

The optimized structures of benzylic cations at the RHF/6–31G* level are shown in Figures 4–7 and their selected geometrical parameters are summarized in

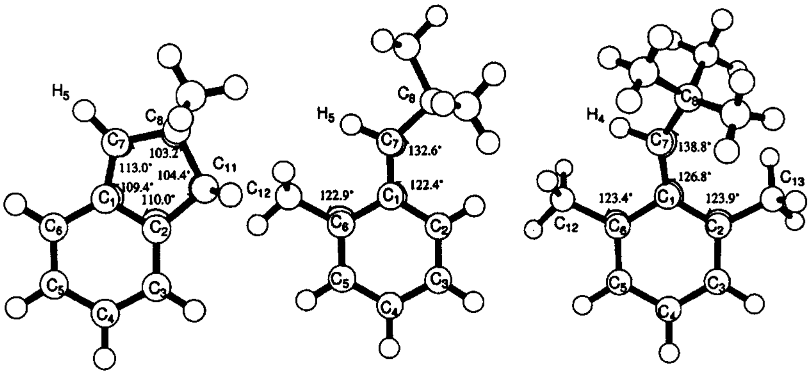

1 4 5

Figure 4. Some other parameters of RHF/6–31G*-optimized structures of **1**, **4** and **5**. See Table 1

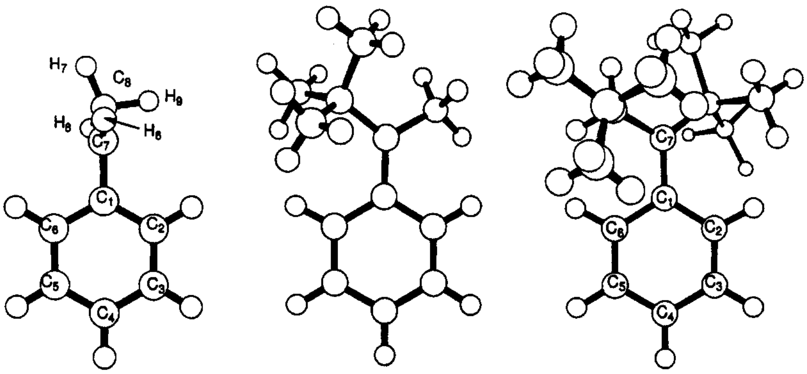

6 11 12

Figure 5. Some other parameters of RHF/6–31G*-optimized structures of **6**, **11** and **12**. See Table 2

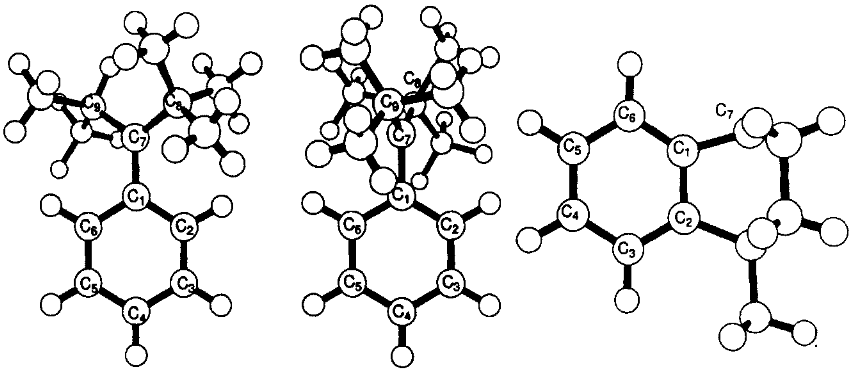

13 14 15

Figure 6. Some other parameters of RHF/6–31G*-optimized structures of **13**–**15**. See Table 3

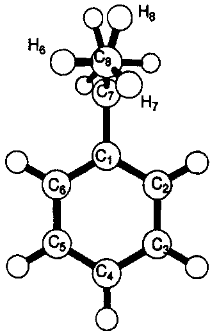

16

Figure 7. Some other parameters of RHF/6–31G*-optimized structure of **16**. See Table 3

Tables 1–3. The calculated dihedral angles $\angle C_2C_1C_7C_6$, $\angle C_1C_2C_3C_4$, $\angle C_2C_3C_4C_5$, $\angle C_3C_4C_5C_6$, $\angle C_4C_5C_6C_1$, $\angle C_5C_6C_1C_2$ and $\angle C_6C_1C_2C_3$ for all benzylic cations without **5** are less than 3·0°, indicating that the phenyl rings of these cations are planar. Thus the dihedral angle ϕ and the electronic effect of α-substituents (R_1, R_2) are considered to be the main factors determining the degree of resonance interaction for these benzylic cations. All stable conformations except 90° fixed cations have only positive vibrational frequencies so that these structures are energy minimum structures at the RHF/6–31G* potential energy surface (PES). Geometries of the individual benzylic cations are discussed below.

2,2-Dimethyl-1-indanyl cation (1)

Cation **1** is converged to a C_s structure for all basis sets (Figure 4). The five-membered ring is coplanar with the benzene framework. Although large steric strain exists in a five-membered ring included in a fused benzene ring ($\angle C_1C_7C_8 = 113{\cdot}0°$, $\angle C_7C_8C_{11} = 103{\cdot}2°$, $\angle C_8C_{11}C_2 = 104{\cdot}4°$, $\angle C_{11}C_2C_1 = 110{\cdot}0°$, $\angle C_2C_1C_7 = 109{\cdot}4°$), the vacant $2p\pi$-orbital on C_7 is parallel to the benzene π system, so the full resonance stabilization can be expected. Actually, YT analysis on the solvolysis of corresponding precursors gave the maximum r value ($r = 1.14$) for secondary systems.[3g]

α-t-Butyl-o-methylbenzyl cation (4)

Cation **4** corresponds to *o*-methyl-substituted **3**. The *t*-Bu group is placed in the opposite side of the *o*-Me group to minimize steric hindrance (Figure 4), so $\phi = 0°$ was obtained for all basis sets.

α-t-Butyl-o,o-dimethylbenzyl cation (5)

The introduction of one more methyl group in **4** is expected to produce a large steric hindrance and to change considerably the dihedral angle ϕ. The structure for **5** optimized at the RHF/6–31G* level is shown in Figure 4. Full resonance stabilization cannot be accomplished owing to the large steric hindrance ($\phi = 19°$). This cation (**5**) minimizes the steric hindrance in a different manner to other tertiary congested systems such as **11**–**14**. The steric hindrance decreased owing not only to the rotation of the *t*-Bu group around the $C_1 - C_7$ axis but also to changes of several dihedral angles ($\angle C_7C_1C_2C_3 = 163.0°$ and $\angle C_1C_2C_3C_4 = 2.9°$). This suggests that the resonance effect attaining a coplanar conformation has a large influence on the stabilization of this secondary cation. The r value in the YT equation for solvolysis leading to **5** has been found to be 1·02,[3f] in addition to $r = 1{\cdot}14$[3g] for that of **1** considering a secondary coplanar system. The decrease in the resonance interaction is only 10%. This may be attributed to the large resonance stabilization effect for secondary systems compared with that for tertiary systems.

Table 1. Selected geometric parameters[a] for **1**, **4** and **5** optimized at the RHF/6–31G* level

	Cation		
	2,2-Dimethyl-1-indanyl (**1**)	α-*t*-Butyl-*o*-methylbenzyl (**4**)	α-*t*-Butyl-*o*,*o*-dimethylbenzyl (**5**)
C_1-C_2	1·424	1·435	1·450
C_2-C_3	1·374	1·359	1·371
C_3-C_4	1·387	1·400	1·392
C_4-C_5	1·411	1·389	1·389
C_5-C_6	1·360	1·379	1·373
C_6-C_1	1·419	1·446	1·457
C_1-C_7	1·369	1·380	1·383
$C_7-R_1^b$	1·498	1·517	1·514
$C_7-R_2^b$	1·074	1·075	1·072
$C_7-C_1-C_2$	109·4	122·4	126·8
$C_7-C_1-C_6$	129·5	118·9	114·3
$C_1-C_7-R_1^b$	113·0	132·6	138·8
$C_1-C_7-R_2^b$	124·8	114·5	112·5
ϕ^c	0	0	19

[a] Distance in angstroms, angle in degrees.
[b] R_1 and R_2 correspond right- and left-hand side atoms bonded to C_7 given in Figure 4, respectively. The numbering of atoms is given in Figure 2.
[c] Average of dihedral angles of $\angle R_1C_7C_1C_2$ and $\angle R_2C_7C_1C_6$.

Table 2. Selected geometric parameters[a] for **6**, **11** and **12** optimized at the RHF/6–31G* level

	Cation		
	α-Methylbenzyl (ϕ = 90° fixed) (**6**)	α-*t*-Butyl-α-methylbenzyl (**11**)	α-*t*-Butyl-α-neopentylbenzyl (**12**)
C_1-C_2	1·391	1·420	1·419
C_2-C_3	1·384	1·373	1·372
C_3-C_4	1·386	1·390	1·392
C_4-C_5	1·386	1·393	1·388
C_5-C_6	1·384	1·371	1·375
C_6-C_1	1·392	1·419	1·418
C_1-C_7	1·466	1·423	1·434
$C_7-R_1^b$	1·082[d]	1·497	1·506
$C_7-R_2^b$	1·450[e]	1·532	1·548
$C_7-C_1-C_2$	119·8	119·3	122·8
$C_7-C_1-C_6$	118·5	123·3	120·5
$C_1-C_7-R_1^b$	118·6	118·7	118·5
$C_1-C_7-R_2^b$	124·0	125·0	122·0
ϕ^c	90	24	26

[a] Distance in angstroms, angle in degrees.
[b] R_1 and R_2 correspond to right- and left-hand side atoms bonded to C_7 given in Figure 5, respectively. The numbering of atoms is given in Figure 2.
[c] Average of dihedral angles of $\angle R_1C_7C_1C_2$ and $\angle R_2C_7C_1C_6$.
[d] Bond length between C_7 and H_6.
[e] Bond length between C_7 and C_8.

Highly congested cations: α-t-butyl-α-methylbenzyl cation (11), α-t-butyl-α-neopentylbenzyl cation (12), α-t-butyl-α-isopropylbenzyl cation (13) and α,α-di-t-butylbenzyl cation (14)

In these cations, the bulkiness of one α-substituent increases stepwise from methyl (**11**) through neopentyl (**12**) and isopropyl (**13**) to *tert*-butyl (**14**) (Figures 5 and 6). These species cannot maintain coplanarity between the $R_1C_7R_2$ plane and the benzene framework; large steric hindrance exists which overwhelms resonance stabilization. As the bulkiness of the α-substituent increases gradually, the dihedral angle ϕ increases; ϕ = 24° for **11**, 26° for **12**, 34° for **13** and 76° for **14**. The values for **11**, **12** and **13** are almost independent of the basis set selections. On the other hand, ϕ for

Table 3. Selected geometric parameters[a] for **13**–**16** optimized at the RHF/6–31G* level

	Cation			
	α-*t*-Butyl-α-isopropylbenzyl (**13**)	α,α-Di-*t*-butylbenzyl (**14**)	4-Methylbenzobicyclo[2.2.2]octen-1-yl (**15**)	α,α-Dimethylbenzyl (ϕ = 90° fixed) (**16**)
C_1–C_2	1·414	1·394	1·402	1·390
C_2–C_3	1·374	1·383	1·380	1·384
C_3–C_4	1·390	1·386	1·392	1·386
C_4–C_5	1·389	1·386	1·384	1·386
C_5–C_6	1·375	1·383	1·390	1·384
C_6–C_1	1·414	1·394	1·377	1·390
C_1–C_7	1·434	1·482	1·470	1·478
C_7–R_1^b	1·533	1·519	1·459	1·468
C_7–R_2^b	1·522	1·519	1·459	1·468
C_7–C_1–C_2	122·2	120·0	105·4	119·3
C_7–C_1–C_6	120·2	120·0	131·4	119·3
C_1–C_7–R_1^b	122·8	117·0	116·2	119·6
C_1–C_7–R_2^b	120·2	117·0	116·2	119·6
ϕ^c	34	76	90	90

[a] Distance in angstroms, angle in degrees.
[b] R_1 and R_2 correspond right- and left-hand side atoms bonded to C_7 given in Figure 6, respectively. The numbering of atoms is given in Figure 2.
[c] Average of dihedral angles of $\angle R_1C_7C_1C_2$ and $\angle R_2C_7C_1C_6$.

14 is somewhat basis set dependent; the configuration of the *t*-Bu group is changed to rotate around the C_7–C_8 and C_7–C_9 axes by only about 5°, but the dihedral angle ϕ increases by 22° with the use of the split valence basis set keeping C_2 symmetry.

Conformationally 90° fixed cation: 4-methylbenzobicyclo[2.2.2]octen-1-yl cation (15)

The geometry of **15** was converged to a C_s structure for all basis sets (Figure 6); the 2pπ-orbital on C_7 is set perpendicular to the benzene π system. This supports the experimental result of $r = 0$ in the solvolysis study.[31]

90° Fixed cations: α,α-dimethylbenzyl cation (ϕ = 90° fixed) (16), α-methylbenzyl cation (ϕ = 90° fixed) (6)

Cations **16** and **6** were optimized under the condition that the angle between the $R_1C_7R_2$ plane and the $C_1C_2C_6$ plane is fixed at 90° (Figures 5 and 7). The carbon–carbon bond lengths of the phenyl rings are in the range 1·38–1·39 Å which is similar to the carbon–carbon bond length of benzene (1·39 Å at the RHF/6–31G* level). Hence these supposed systems are not stabilized by the resonance interaction between C_7 and the benzene π system.

The configurations of methyl groups for **16** and **6** are instructive. In **6**, the C_8 – H_9 bond is parallel with the vacant 2pπ orbital at $C_7(\angle H_9C_8C_7C_1 = 92°)$. Such a configuration cannot be found in the coplanar cation **2**. Moreover, $\angle H_9C_8C_7$ is 100·4° which is smaller than the normal tetrahedral angle. This result might be attributed to C–H hyperconjugation. For the hypothetical localized cation **16**, the effect of hyperconjugation is also expected. As expected, the C_8 – H_6 bond is almost parallel to the benzylic 2pπ-orbital $(\angle H_6C_8C_7C_1 = 81{\cdot}9°)$, but slightly twisted owing to steric repulsion between two methyl groups. $\angle H_6C_8C_7 (= 103{\cdot}0°)$ is smaller than the usual tetrahedral angle, but slightly larger than that in **6**, owing to dispersional interaction between two methyl groups. The positive charge is delocalized largely into the benzene π system in coplanar systems, so that the hyperconjugative stabilization is relatively small compared with that for a localized one. However, for cations **16** and **6**, the positive charge at C_7 localizes in the non-aromatic moiety similar to a simple alkyl cation. In this case, hyperconjugation becomes significant. It should be noted that $\angle H_6C_8C_7$ and $\angle H_7C_8C_7$ are 103·0° and 113·7°, respectively, which are values between sp^2 and sp^3 hybridization. This is the reason why $\angle H_9C_8C_7$ (= 100·4°) in **6** is smaller than the 109·5° for sp^3 hybridization.

The energy difference between these 90° fixed cations (**16** and **6**) and the corresponding coplanar cations (**7** and **2**) can be approximated to the rotational potential barriers around the C_1 – C_7 axis. Normal mode analysis in the frequency calculation indicates that **16** and **6** are transition states concerning rotation of the C_1 – C_7 axis, because they have one imaginary vibrational frequency. In addition, the perpendicular conformation is energetically maximum among all of the rotamers for the benzyl cation,[8] whereas some steric effect may exist for the coplanar structure of **7**, resulting in a small dihedral angle ($\phi = 5°$).[1] The rotational potential barriers for each cation are sum-

Table 4. Calculated rotational barriers[a] (kcal mol^{-1}) of benzylic cations at various basis sets

Cations	RHF/STO-3G	RHF/3-21G	RHF/6-31G*	MP2/6-31G*//RHF/6-31G*
Benzyl	47·1	45·4[b]	45·9	49·3
α-Methylbenzyl	34·5	31·8	32·4	33·8
α,α-Dimethylbenzyl	22·0	19·0	19·7	20·7

[a] Rotational barriers were estimated as the total energy difference between coplanar and orthogonal ($\phi = 90°$) optimized structures: E(**16**) – E(**7**) for α,α-dimethylbenzyl cation and E(**6**) – E(**2**) for α-methylbenzyl cation.

[b] Ref. 8.

marized in Table 4. Basis sets and electron correlation do not seriously affect the barriers. With MP2/6–31G*//RHF/6–31G* calculation, the potential barriers are 49·3 kcal mol^{-1} for benzyl cation, 33·8 kcal mol^{-1} for α-methylbenzyl cation and 20·7 kcal mol^{-1} for α,α-dimethylbenzyl cation, respectively (1 kcal = 4·184 kJ). The rotational barrier has been used as a measure of the 'resonance interaction energy'.[9] One methyl substitution at the benzylic position lowers the rotational barrier by *ca* 15 kcal mol^{-1}. This may be attributed to the difference between the resonance stabilization of each benzylic cation. The primary benzyl cation is required to have larger conjugation in order to stabilize the total energy. On the other hand, the tertiary α,α-dimethylbenzyl cation (**7**) is stabilized by the electronic effect of the α-methyl group, so that the requirement for resonance stabilization is small. Although the energy difference may contain a little steric repulsion, it is worth noting that the r value in the YT equation runs parallel with the rotational barriers of the corresponding benzylic cations. This is instructive, because the r value can be connected to the resonance interaction energy.

ϕ Dependence of the r values estimated from solvolyses

As reported in Part 1,[1] the Wiberg bond order of the $C_1 - C_7$ bond for benzylic cations increases linearly with increase in the resonance demand r. This suggests that the r value might also be closely related to the degree of π overlapping between the aryl π-orbital and benzylic 2pπ-orbital in the carbocation (Figure 1). Accordingly, the dihedral angle ϕ and the r value might be related each other. The dependence of the r value on the dihedral angle ϕ can be expressed as follows:

$$r/r_{\max} = f(\phi) \qquad (2)$$

where r and $r_{\max}$ are the effective resonance interaction of any given system examined and the corresponding ideal full-resonance stabilized interaction, respectively, and $f(\phi)$ is a function of the dihedral angle ϕ. According to the HMO method, this function can be expressed analytically for the resonance energy of benzylic cations as shown below. In the HMO method, when we put the resonance integrals as follows:

$$\beta_{17} = \beta \cos\,\phi, \quad \beta_{12} = \beta_{23} = \beta_{34} = \beta_{45} = \beta_{56} = \beta_{16} = \beta \qquad (3)$$

The secular determinant can be written as

$$\begin{vmatrix} x & k & 0 & 0 & 0 & 0 & 0 \\ k & x & 1 & 0 & 0 & 0 & 1 \\ 0 & 1 & x & 1 & 0 & 0 & 0 \\ 0 & 0 & 1 & x & 1 & 0 & 0 \\ 0 & 0 & 0 & 1 & x & 1 & 0 \\ 0 & 0 & 0 & 0 & 1 & x & 1 \\ 0 & 1 & 0 & 0 & 0 & 1 & x \end{vmatrix}$$

$$\begin{aligned} &= x(x^2 - 1)[x^4 - (5 + k^2)x^2 + 4 + 3k^2] \\ &= x(x + 1)(x - 1)(x + \sqrt{10 + 2k^2 + 2\sqrt{9 - 2k^2 + k^4}}/2) \\ &\quad \times (x - \sqrt{10 + 2k^2 + 2\sqrt{9 - 2k^2 + k^4}}/2) \\ &\quad \times (x + \sqrt{10 + 2k^2 - 2\sqrt{9 - 2k^2 + k^4}}/2) \\ &\quad \times (x - \sqrt{10 + 2k^2 - 2\sqrt{9 - 2k^2 + k^4}}/2) \end{aligned} \qquad (4)$$

where $x = (\alpha - E)\beta$ and $k = \cos\,\phi$. Therefore, the HMO energies are

$$\begin{aligned} E_1 &= \alpha + \sqrt{10 + 2k^2 + 2\sqrt{9 - 2k^2 + k^4}}\,\beta/2 \\ E_2 &= \alpha + \sqrt{10 + 2k^2 - 2\sqrt{9 - 2k^2 + k^4}}\,\beta/2 \\ E_3 &= \alpha + \beta \\ E_4 &= \alpha \end{aligned}$$

The ϕ dependence of the energy for resonance interaction, $\Delta E_{\mathrm{R}}(\phi)$, can be given as

$$\begin{aligned} \Delta E_{\mathrm{R}}(\phi) &= E(\phi) - E(\phi = 90°) \\ &= (\sqrt{10 + 2\cos^2\phi + 2\sqrt{\sin^4\phi + 8}} \\ &\qquad + \sqrt{10 + 2\cos^2\phi - 2\sqrt{\sin^4\phi + 8}} - 6)\beta \end{aligned} \qquad (5)$$

$$\Delta E_{\mathrm{R}}(\phi = 0) = (\sqrt{12 + 2\sqrt{8}} + \sqrt{12 - 2\sqrt{8}} - 6)\beta \qquad (6)$$

Therefore, $f_1(\phi)$ is expressed by

$$\begin{aligned} f_1(\phi) &= \Big(\sqrt{10 + 2\cos^2\phi + 2\sqrt{\sin^4\phi + 8}} \\ &\quad + \sqrt{10 + 2\cos^2\phi - 2\sqrt{\sin^4\phi + 8}} - 6\Big)/ \\ &\quad \Big(\sqrt{12 + 2\sqrt{8}} + \sqrt{12 - 2\sqrt{8}} - 6\Big) \\ &= \cos^2\phi + \Delta \qquad (0 \leqslant \Delta \leqslant 0{\cdot}0356) \qquad (7) \end{aligned}$$

Hence we can express $f_1(\phi)$, to a good approximation, as

$$f_1(\phi) = \cos^2\phi \qquad (8)$$

In this paper,

$$f_2(\phi) = \cos\phi \qquad (9)$$

has been also considered in discussion for comparison.

For *ab initio* MO calculations, the resonance interaction energy $\Delta E_R^{SCF}(\phi)$ is given by the negative SCF energy at the RHF/6–31G* level relative to that of the 90° fixed cation. Hence

$$\Delta E_R^{SCF}(\phi) = \Delta E_R^{SCF}(\phi) - \Delta E_R^{SCF}(\phi = 90°) \qquad (10)$$

The $\Delta E_R^{SCF}(\phi)$ values of the benzyl cation were calculated and plotted against $f_1(\phi)$ and $f_2(\phi)$ as shown in Figure 8. As can be seen, the best expression for $f(\phi)$ may be

$$f(\phi) = \cos^{1.8}\phi$$

However, for practical purposes,

$$r/r_{max} = \cos^2\phi \qquad (11)$$

is recommended.

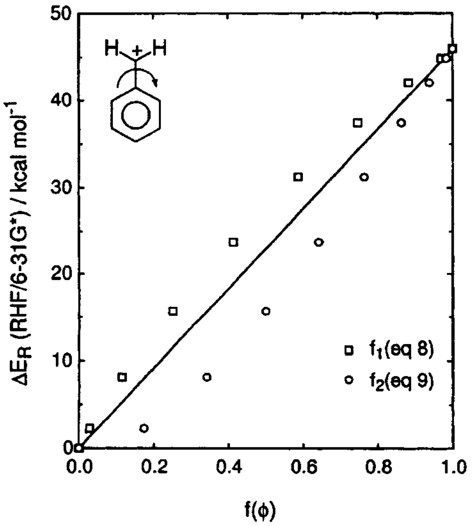

Figure 8. Calculated delocalization energies of benzyl cations at the RHF/6–31G* level. $\Delta E_R^{SCF} = \Delta E^{SCF}(\phi) - \Delta E^{SCF}(\phi = 90°)$. □, $f_1(\phi)$; ○, $f_2(\phi)$

Relationships between calculated dihedral angle ϕ_{calc} and *r* value

Assuming the α,α-dimethylbenzyl cation to be coplanar, its *r* value may be regarded as a reference r_{max} value of a coplanar tertiary carbocation, because the *r* value is characterized by 1·0 for planar α,α-dialkyl (tertiary) benzyl cations.[4e] As shown in Table 5, *r* values estimated from solvolysis and gas-phase cations agree with each other, to a first approximation, suggesting intrinsically identical structures between the transition state and corresponding cation. As shown in Figure 9, there is a linear correlation between $\cos^2\phi_{calc}$ calculated at the RHF/6–31G* level and the r/r_{max} values for tertiary benzylic cations.

One may be interested in examining the effect of electron correlation on the resonance interaction for congested systems. Unfortunately, geometry optimization at the MP2 or higher levels of theory take a long time so MP2 calculations for these bulky systems have not yet been performed. In this paper, in order to discuss the effect of electron correlation on the dihedral angle ϕ, single-point calculations at the MP2 level for **7**, **11**, **12**, **13** and **14** were carried out with the geometry where the dihedral angle ϕ changes by ±5° around the $C_1 - C_7$ axis from the RHF/6–31G*-optimized geometry. The energy differences between the structure of each dihedral angle and the optimized one are plotted in Figure 10. The plots for all cations are correlated by quadratic equations. As shown in Figure 10, the correlation curve without **14** is symmetrical with respect to the equilibrium ϕ at the RHF/6–31G* level; electron correlation has very small effect on the optimized structure. For **14**, single-point calculation extended to the ϕ which is swung by −10°, since a monotonic potential curve was obtained for these three plots ($\theta = \pm 5°$). As a result, an unsymmetric curved plot was obtained; electron correlation cannot be neglected for the accurate determination of the structure of this congested cation. This supports the result of a failed plot for **14** (open circle) in Figure 9. The minimum ϕ for **14** was calculated to be 71° on the assumption of a multi-regression correlation, that is, the electron correlation effect decreases ϕ by 5°. Consequently, an electron correlation effect exists for the dihedral angle of this cation, although the effect is not large. In the case of **14**, optimization at the MP2/6–31G* level, which can estimate the electron correlation effect, was also performed with C_2 symmetry. The dihedral angle ϕ_{calc} was calculated to be 69°, which is consistent with the above result and gives a more accurate plot (closed circle for **14**) in Figure 9.

For secondary systems, ϕ_{calc}, *r* values, r/r_{max} and $\cos^2\phi_{calc}$ calculated at the RHF/6–31G* level are summarized in Table 6. The 2,2-dimethyl-1-indanyl system (**1**) is a coplanar standard of the secondary system. The ϕ values do not change drastically com-

Table 5. Calculated dihedral angles ϕ_{calc}[a] for tertiary benzylic cations and r values

Cation	ϕ_{calc} RHF/STO-3G	RHF/3-21G	RHF/6-31G*	MP2/6-31G*	r_{sol}[b]	r_{gas}[c]	$r_{max}\cos^2 \phi_{calc}$
7	0	5	5	7[d]	1·00	1·00[l]	0·99
8	2	2	3	2[d]	1·04[f]	1·01[m]	1·00
9	1	1	0		1·02[g]		1·00
10	10	11	10		1·01[f]		0·97
11	20	24	24		0·91[h]	0·86[n]	0·83
12	21	32	26		0·78[g]	0·81[g]	0·81
13	31	37	33		0·71[i]		0·70
14	55	77	76	69[e]	0·26[j]		0·06
15	90	90	90		0[k]		0·00

[a] See Figure 2.

[b] The r value given in the solvolysis of each system.

[c] The r value given in the gas-phase stabilities of each system.

[d] MP2(FULL).

[e] Frozen core approximation.

[f] Ref. 3h.

[g] Unpublished results in this laboratory.

[h] Ref. 3i.

[i] Ref. 3j.

[j] Ref. 3k.

[k] Ref. 3l.

[l] Ref. 4a.

[m] Ref. 4e.

[n] Ref. 4g.

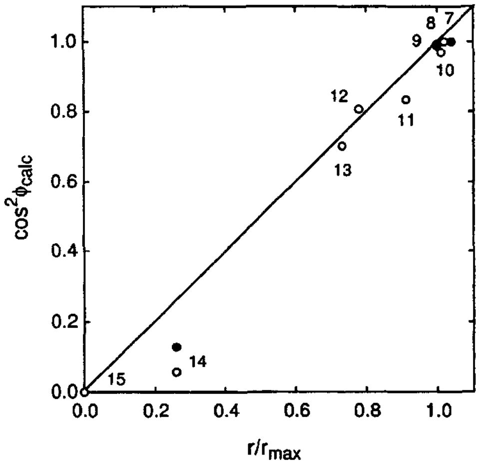

Figure 9. Plots of $\cos^2 \phi_{calc}$ vs r/r_{max}. Open and closed circles are plots calculated at the RHF/6-31G* and MP2/6-31G* levels, respectively. Numbers correspond to those for cations shown in Figure 3

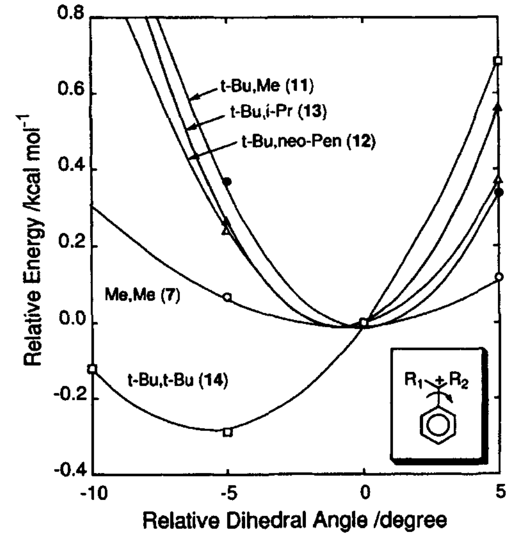

Figure 10. Plot of energies with MP2 single-point calculation relative to that of RHF/6-31G*-optimized structure for congested cations. Relative dihedral angles to the optimized structure at the RHF/6-31G* level are taken for the abscissa

Table 6. Calculated dihedral angles ϕ_{calc}[a] for secondary benzylic cations, r values and $r/r_{max}\cos^2\phi_{calc}$ values calculated at the RHF/6-31G* level

	ϕ_{calc}				
Cation	RHF/STO-3G	RHF/3-21G	RHF/6-31G*	r_{sol}[b]	$r_{max}\cos^2\phi_{calc}$
1	0	0	0	1·14[c]	1·15
2			0	1·15[d]	1·15
3	0	0	0	1·09[e]	1·15
4	0	0	0	1·01[f]	1·15
5	16	25	22	1·02[f]	0·99

[a] See Figure 2.
[b] The r value given in the solvolysis of each system.
[c] Ref. 3g.
[d] Ref. 3d.
[e] Ref. 3e.
[f] Ref. 3f.

pared with those for tertiary systems. This may be attributed intrinsically to the large resonance demand of secondary systems. The r/r_{max} and $\cos^2\phi_{calc}$ values agree fairly well with each other.

These results for secondary and tertiary cations indicate that the r value is a good parameter associated with the degree of resonance interaction.

ACKNOWLEDGEMENTS

This work was supported by a Grand-in-Aid for Developmental Scientific Research from the Ministry of Education, Science and Culture, Japan.

REFERENCES

1. K. Nakata, M. Fujio, Y. Saeki, M. Mishima, Y. Tsuno and K. Nishimoto, *J. Phys. Org. Chem.* **9**, 561–572 (1996).
2. Y. Yukawa and Y. Tsuno, *Bull. Chem. Soc. Jpn.* **32**, 971–981 (1959); Y. Yukawa, Y. Tsuno and M. Sawada, *Bull. Chem. Soc. Jpn.* **39**, 2274–2286 (1966).
3. (a) A. Murata, M. Goto, R. Fujiyama, M. Mishima, M. Fujio and Y. Tsuno, *Bull. Chem. Soc. Jpn.* **63**, 1129–1137 (1990); (b) A. Murata, S. Sakaguchi, R. Fujiyama, M. Fujio and Y. Tsuno, *Bull. Chem. Soc. Jpn.* **63**, 1138–1145 (1990); (c) M. Fujio, M. Goto, T. Susuki, I. Akasaka, M. Mishima and Y. Tsuno, *Bull. Chem. Soc. Jpn.* **63**, 1146–1153 (1990); M. Fujio, M. Goto, T. Susuki, M. Mishima and Y. Tsuno, *J. Phys. Org. Chem.* **3**, 449–455 (1990); (d) Y. Tsuno, Y. Kusuyama, M. Sawada, T. Fujii and Y. Yukawa, *Bull. Chem. Soc. Jpn.* **48**, 3337–3346 (1975); M. Fujio, T. Adachi, Y. Shibuya, A. Murata and Y. Tsuno, *Tetrahedron Lett.* **25**, 4557–4560 (1984); (e) Y. Tsuji, M. Fujio and Y. Tsuno, *Bull. Chem. Soc. Jpn.* **63**, 856–866 (1990); (f) M. Fujio, Y. Tsuji, T. Otsu and Y. Tsuno, *Tetrahedron Lett.* **32**, 1805–1808 (1991); (g) M. Fujio, K. Nakata, Y. Tsuji, T. Otsu and Y. Tsuno, *Tetrahedron Lett.* **33**, 321–324 (1992); (h) M. Fujio, K. Nakata, T. Kuwamura, H. Nakamura, Y. Saeki, M. Mishima, S. Kobayashi and Y. Tsuno, *Tetrahedron Lett.* **34**, 8309–8312 (1993); (i) M. Fujio, H. Nomura, K. Nakata, Y. Saeki, M. Mishima, S. Kobayashi, T. Matsushita, K. Nishimoto and Y. Tsuno, *Tetrahedron Lett.* **35**, 5005–5008 (1994); (j) M. Fujio, M. Ohe, K. Nakata and Y. Tsuno, to be published; (k) M. Fujio, T. Miyamoto, Y. Tsuji and Y. Tsuno, *Tetrahedron Lett.* **32**, 2929–2932 (1991); (l) M. Fujio, K. Nakashima, E. Tokunaga, Y. Tsuji and Y. Tsuno, *Tetrahedron Lett.* **33**, 345–348 (1992).
4. (a) M. Mishima, H. Inoue, M. Fujio and Y. Tsuno, *Tetrahedron Lett.* **30**, 2101–2104 (1989); (b) M. Mishima, H. Inoue, M. Fujio and Y. Tsuno, *Tetrahedron Lett.* **31**, 685–688 (1990); (c) M. Mishima, K. Arima, S. Usui, M. Fujio and Y. Tsuno, *Mem. Fac. Sci., Kyushu Univ., Ser. C* **15**, 277–286 (1986); M. Mishima, K. Arima, S. Usui, M. Fujio and Y. Tsuno, *Chem. Lett.* 1047–1050 (1987); (d) M. Mishima, S. Usui, M. Fujio and Y. Tsuno, *Nippon Kagaku Kaishi* 1269–1274 (1989); (e) M. Mishima, H. Nakamura, K. Nakata, M. Fujio and Y. Tsuno, *Chem. Lett.* 1607–1610 (1994); (f) M. Mishima, S. Usui, H. Inoue, M. Fujio and Y. Tsuno, *Nippon Kagaku Kaishi* 1262–1268 (1989); (g) M. Mishima, K. Nakata, H. Nomura, M. Fujio and Y. Tsuno, *Chem. Lett.* 2435–2438 (1992); K. Nakata, H. Nomura, M. Mishima, Y. Saeki, K. Nishimoto, T. Matsushita, M. Fujio and Y. Tsuno, *Mem. Fac. Sci., Kyushu Univ., Ser. C* **18**, 287–296 (1992).
5. W. J. Hehre, L. Radom, P. v. R. Schleyer and J. A. Pople, *Ab Initio Molecular Orbital Theory.* Wiley, New York (1986).
6. M. J. Frisch, G. W. Trucks, M. Head-Gordon, P. M. W. Gill, M. W. Wong, J. B. Foresman, B. G. Johnson, H. B. Schlegel, M. A. Robb, E. S. Replogle, R. Gemperts, J. L. Andres, K. Raghavachari, J. S. Binkley, C. Gonzalez, R. L. Martin, D. J. Fox, D. J. DeFrees, J. Baker, J. J. P. Stewart and J. A. Pople, *Gaussian 92*. Gaussian, Pittsburgh, PA (1992).
7. C. Møller and M. S. Plesset, *Phys. Rev.* **46**, 618–622 (1934).
8. A. E. Dorigo, Y. Li and K. N. Houk, *J. Am. Chem. Soc.* **111**, 6942–6948 (1989).
9. H. Mayr, W. Forner and P. v. R. Schleyer, *J. Am. Chem. Soc.* **101**, 6032–6040 (1979).